Stabilization of Labile Carbonyl Addition Intermediates by a Synthetic Receptor

Tetsuo Iwasawa, *et al.*

Science **317**, 493 (2007);
DOI: 10.1126/science.1143272

Science (print ISSN 0036-8075; online ISSN 1095-9203) is published weekly, except the last week in December, by the American Association for the Advancement of Science, 1200 New York Avenue NW, Washington, DC 20005.

contaminated by 645 parts per million (ppm) Hg^{2+}, 10 mg of Chalcogel-1 removed Hg^{2+} down to concentration levels of ~0.04 ppm (*14*). Whereas mesoporous silicates need to be functionalized with surface-modified thiolate ligands before application toward environmental remediation (*15*), the chalcogels work directly as potential adsorbents for Hg^{2+} (*16*) without prior modification of their surface. The detailed mechanism of metal ion removal is not known.

The chalcogels also efficiently absorb organic hydrophobic aromatic molecules from solution. In contrast to the unmodified silica aerogels—which generally have hydrophilic surfaces and tend to be unstable under a humid atmosphere—the chalcogels present hydrophobic surfaces lined with chalcogen atoms and are immune to high humidity (*17*). Thermal gravimetric analysis indicates that the aerogels are stable to 180°C (fig. S6). As a demonstration of its high affinity for hydrophobic species, Chalcogel-1 absorbed quantitatively all of porphyrin I from a 5.67 μmol/liter ethanolic solution within 24 hours (30 mg of Chalcogel-1 was shaken continuously in 16 ml of the porphyrin solution).

The chalcogels absorb light in the visible and infrared regions, exhibiting sharp energy gaps from 2.0 eV to 0.8 eV (Table 1) as determined by diffuse-reflectance solid-state ultraviolet-visible/near-infrared spectroscopy (Fig. 4C). Only Chalcogel-5 gave a broad absorption with a band gap of 0.2 eV. The optical properties of the highly porous semiconducting aerogels can be tuned by changing the building block. Going from the S to the Se analogs of the adamantane cluster, the energy gap decreases as expected. Also, by changing the group IV metal in the cluster from Ge to Sn, the energy gap is decreased by 0.3 eV. Similarly, the band gap can also be changed by varying the chalcogenide content per metal in the starting clusters. This is well reflected in the observed band gaps of Chalcogel-3, -4, and -5, where the Se content per Sn atom is increased gradually and shows a narrowing of the energy gap.

Given that it is difficult to remove surfactants from mesostructured chalcogenide materials (*18*–*22*), the strategy reported here represents a convenient and general route for making porous materials with chalcogenide-based clusters. Because of the availability of a large number of soluble chalcogenido clusters, together with various linking transition and main-group metal ions, our approach seems to offer a general technique for preparing broad classes of porous chalcogenides.

References and Notes

1. X. He, D. Antonelli, *Angew. Chem. Int. Ed.* **41**, 214 (2002).
2. M. A. Carreon, V. V. Guliants, *Eur. J. Inorg. Chem.* **2005**, 27 (2005).
3. C. J. Brinker, G. W. Scherer, *The Physics and Chemistry of Sol-Gel Processing* (Academic Press, San Diego, CA, 1990).
4. N. Hüsing, U. Schubert, *Angew. Chem. Int. Ed.* **37**, 22 (1998).
5. R. W. Pekala, C. T. Alviso, F. M. Kong, S. S. Hulsey, *J. Non-Cryst. Solids* **145**, 90 (1992).
6. J. L. Mohanan, I. U. Arachchige, S. L. Brock, *Science* **307**, 397 (2005).
7. K. K. Kalebaila, D. G. Georgiev, S. L. Brock, *J. Non-Cryst. Solids* **352**, 232 (2006).
8. See supporting material on *Science* Online.
9. M. Heibel, G. Kumar, C. Wyse, P. Bukovec, A. B. Bocarsly, *Chem. Mater.* **8**, 1504 (1996).
10. S. S. Kistler, *J. Phys. Chem.* **36**, 52 (1932).
11. S. J. Gregg, K. S. W. Sing, *Adsorption, Surface Area and Porosity* (Academic Press, New York, 1982).
12. The molecular formulas were normalized to two sulfur or two selenium atoms to compare well with SiO_2 (e.g., $Pt_2Ge_4S_{10}$ is converted to $Pt_{0.4}Ge_{0.8}S_2$ having formula weight of 220.27) for equivalent surface area calculation.
13. S. J. L. Billinge, M. G. Kanatzidis, *Chem. Commun.* **2004**, 749 (2004).
14. The capacity of Chalcogel-1 to remove Hg^{2+} from aqueous solution is extremely high (645 mg/g or 3.21 mmol/g). This tremendous affinity is also reflected in the calculated distribution coefficient K_d^{Hg} [defined as the amount of adsorbed metal (in micrograms) on 1 g of adsorbing material divided by the metal concentration (in milligrams per milliliter) remaining in the treated water (*8*)]. K_d^{Hg} values varied from 0.92×10^7 ml/g (at 92 ppm Hg^{2+}) to 1.61×10^7 ml/g (at 645 ppm Hg^{2+}).
15. L. Mercier, T. J. Pinnavaia, *Adv. Mater.* **9**, 500 (1997).
16. The specific binding of chalcogels with heavy metals was demonstrated by adding 5 ml each of 89 ppm Zn^{2+} and 92 ppm Hg^{2+} solutions to 10 mg Chalcogel-2 and stirring for 24 hours at room temperature. The final solution contained 52.8 ppm Zn^{2+} and 0.1 ppm Hg^{2+}.
17. The BET surface area remained high after storing the chalcogels for longer times. For example, the surface area of Chalcogel-2 decreased from 327 to 303 m^2/g after 5 weeks and to 265 m^2/g after 3 months.
18. M. J. MacLachlan, N. Coombs, G. A. Ozin, *Nature* **397**, 681 (1999).
19. P. N. Trikalitis, K. K. Rangan, T. Bakas, M. G. Kanatzidis, *Nature* **410**, 671 (2001).
20. P. N. Trikalitis, K. K. Rangan, M. G. Kanatzidis, *J. Am. Chem. Soc.* **124**, 2604 (2002).
21. P. N. Trikalitis, K. K. Rangan, T. Bakas, M. G. Kanatzidis, *J. Am. Chem. Soc.* **124**, 12255 (2002).
22. S. D. Korlann, A. E. Riley, B. L. Kirsch, B. S. Mun, S. H. Tolbert, *J. Am. Chem. Soc.* **127**, 12516 (2005).

23. We thank T. J. Pinnavaia and D. Holmes for use of the nitrogen sorption measurement and NMR handling, respectively. Use of the Advanced Photon Source was supported by the U.S. Department of Energy, Office of Science, Office of Basic Energy Sciences.

Supporting Online Material

www.sciencemag.org/cgi/content/full/317/5837/490/DC1
Materials and Methods
Figs. S1 to S6
References

14 March 2007; accepted 5 June 2007
10.1126/science.1142535

Stabilization of Labile Carbonyl Addition Intermediates by a Synthetic Receptor

Tetsuo Iwasawa, Richard J. Hooley, Julius Rebek Jr.*

Products of unfavorable chemical equilibria are not readily observed because their high energy and increased reactivity result in low concentrations. Biological macromolecules use binding forces to access unfavorable equilibria and stabilize reactive intermediates by isolating them from the medium. In a similar vein, we describe here a synthetic receptor that allows direct observation of labile tetrahedral intermediates: hemiaminals formed in the reaction of an aldehyde carbonyl group with amines. The receptor encapsulates alkyl-substituted primary amines, then orients them toward a covalently tethered aldehyde function. The hemiaminal intermediates appear at high concentration, confined from the bulk solution and observable at ambient temperature by conventional nuclear magnetic resonance spectroscopy.

Chemical reactions often proceed through many intermediate stages between starting materials and products. The reactive intermediates at such stages are generally not observed directly, because their concentrations are vanishingly small, but are treated through steady-state approximations and detected by kinetic or other methods (*1*, *2*). The reaction of carbonyl compounds with nucleophiles invariably involves an addition step that gives an unstable tetrahedral carbon intermediate followed by an elimination step. For example, the reaction of primary amines with aldehydes to give imines (Fig. 1) proceeds through an intermediate hemiaminal (*3*). The process is catalyzed by acids or bases, and the proton transfers involved generate additional transient, charged intermediates. The hemiaminal is, except in very special cases (*4*–*6*), not observed. It is energetically disfavored, because the cost of breaking the carbonyl π bond and the entropic price of bringing the two reactants together are not compensated by the new covalent bonds formed. Accordingly, the unstable hemiaminal dissociates to starting materials or proceeds to imine with loss of water. We tailored a molecular receptor to favor formation of this intermediate and found that the hemiaminal was stabilized for minutes to hours, long

Skaggs Institute for Chemical Biology and Department of Chemistry, Scripps Research Institute, 10550 North Torrey Pines Road, La Jolla, CA 92037, USA.

*To whom correspondence should be addressed. E-mail: jrebek@scripps.edu

enough to characterize by nuclear magnetic resonance (NMR) spectroscopic methods.

We chose as a receptor motif a deep, self-folding cavitand. Cavitands are open-ended structures that recognize and reversibly bind molecules of appropriate size, shape, and chemical complementarity (*7*, *8*). Synthetic receptors such as these are well known to screen unstable species from the external medium and prolong their lifetimes (*9*–*14*). Examples include the isolation of iminium ions (*9*) and siloxanes (*11*) from the surrounding aqueous environment. In these cases, the receptor functions solely as a shield, protecting the kinetically stable but water-sensitive guest from reaction with the outside medium. Enzymes, in contrast, stabilize kinetically labile intermediates by providing functional groups that actively lower the energy of a bound transition state, via hydrogen bonding or other weak intermolecular forces. The cavitand is in several ways reminiscent of an enzyme active site, comprising a hydrophobic cavity, a secondary amide scaffold, and inwardly directed functional groups folded around the substrate. Detection and analysis of reactive intermediates in biological systems is essential for the accurate determination of enzyme mechanism, but the high activity of enzymes has made such observations difficult. X-ray crystallographic analysis of tetrahedral intermediates inside the active site of D-2-deoxyribose-5-phosphate (DRP) aldolase has been possible at cryogenic temperatures or via selective mutation to prevent the enzyme from completing the reaction (*15*, *16*). The system we describe here is similar in action to a mutant DRP aldolase in which only the first half of the amine-catalyzed aldol reaction occurs. The difference is that the stabilization of the kinetically unstable hemiaminal occurs at room temperature in millimolar concentrations; our system does not require cryogenic cooling in order to observe the intermediate. In certain cases, the intermediate hemiaminal species is observable for more than 3 hours.

We prepared cavitand **1** by the condensation of known diamine **2** (*17*) and dialdehyde **3** using air as the oxidant (Fig. 2) (*18*). The cavity of **1** is large enough to surround a single small molecule guest and orient it toward an inwardly directed aldehyde group. The eight benzene rings act as a fixed solvent cage, and the intramolecular hydrogen bonds of the secondary amides help maintain the vase-like conformation (*19*). When isobutyl amine is added to a solution of **1** in mesitylene-d_{12} (a solvent that does not compete for cavitand binding), a complex forms upon mixing. The ^{1}H NMR spectra (Fig. 3 and figs. S2 to S9) show features typical of binding. Separate sets of resonances are observed for free and encapsulated amine (figs. S2 to S9), because the rates of guest exchange in and out of the host capsules are slow on the NMR time scale. In addition, the amine chemical shifts reflect the orientation in the cavity: The resonances of the apolar CH_3 groups of the bound amine guests show large upfield shifts [$\Delta\delta$ = –4 parts per million (ppm)], consistent with their positioning near the bottom of the cavity, where the many aromatic rings create a magnetically shielded environment. Likewise, polar functions of the guests are attracted to the seam of hydrogen bond donors and acceptors at the rim of the cavitand. Within 2 min of mixing, both the surrounded amine **4** and the corresponding hemiacetal **5** are evident in the spectra. The tetrahedral intermediate **5** (with the hemiaminal proton resonance at 4.6 ppm) shows a half-life ($t_{1/2}$) of 30 min and gradually undergoes dehydration to the imine **6**. The different complexes display peaks for both cavitand and guest with different shifts, leading to rather complex spectra. Figure 3 shows the change in three of these peaks over time; benzimidazole proton H_a (Fig. 2) is the most representative cavitand-based signal because it is distant from the other NH peaks, so the changes are easily visible. The most relevant guest peaks are the terminal CH_3 groups of the amine. The arrangement of hydrogen bonds around the rim of the cavity of **1** creates an asymmetric magnetic environment that is stable on the NMR chemical shift time scale. As a result, the amine methyl groups become diastereotopic upon confinement inside the cavity (even before covalent attachment and hemiaminal formation) and so exhibit separate NMR signals. Each complex shows two different doublets for these methyl groups (the signal for one methyl in complex **4** is buried beneath the hemiaminal signal δ = –3.29). The chemical shift of these methyl groups is dependent on their position in the cavitand base; the deepest bound methyls exhibit the most upfield shift. In the noncovalent complex **4** and the hemiaminal **5**, one of the methyls is positioned deeper inside the cavity than the other, and their resonances are separated by 0.2 ppm. In the case of imine product **6**, the methyl groups are less separated, and the two doublets are overlapped and appear similar to a triplet. The splitting of the signal for the C-H bond of the hemiaminal reflects the formation of a new asymmetric center (and hence two diastereomers) and the large (12 Hz) vicinal coupling to the remaining hydrogen of the amine (no coupling is seen to the OH). A view down the C-N bond (**7**) is shown in Fig. 4A. Hemiaminals were also observed within **1** by using isopropylamine, *n*-propylamine, and *n*-butylamine (figs. S6 to S9). In the latter two cases, the initial

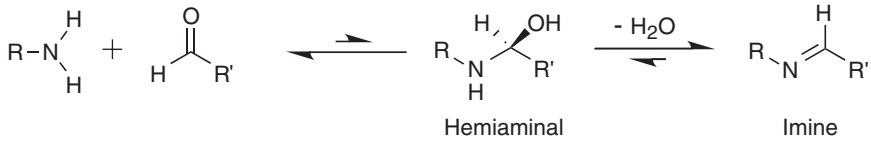

Fig. 1. Mechanism of imine formation from a primary amine and aldehyde. Charged intermediates are not shown.

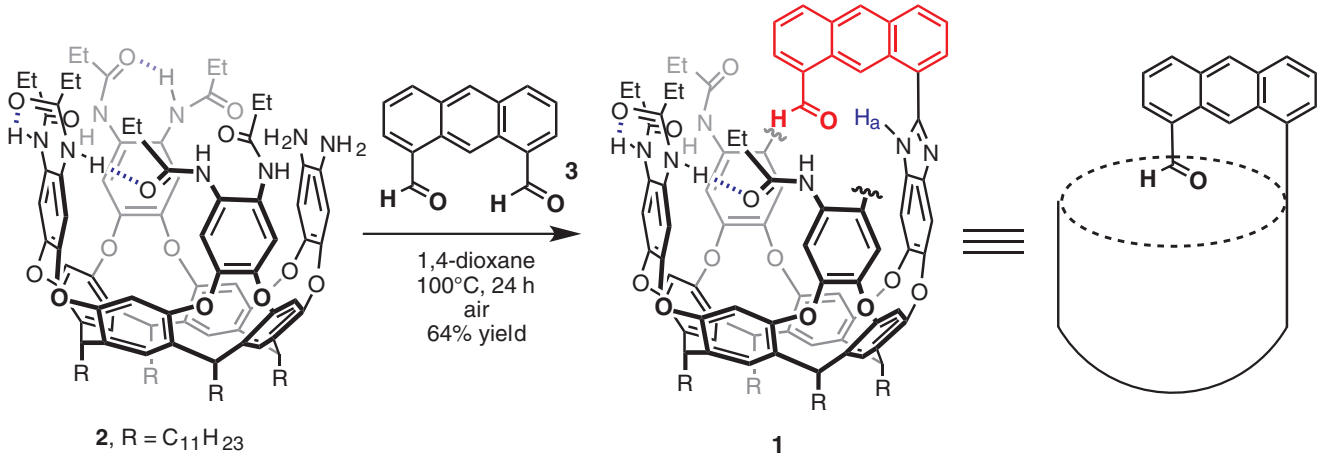

Fig. 2. Synthesis of cavitand **1**. Some peripheral groups were removed for clarity. Et, ethyl group.

noncovalent complexes were too short-lived to observe, and only hemiaminal and imine were seen. The isopropylamine hemiaminal was the longest lived, with a $t_{1/2}$ = 90 min.

Unstabilized hemiaminals have previously been observed very infrequently and only under specialized conditions of highly polar solvents, derivatized starting materials, and high concentrations (*4*–*6*). Our control experiments in the absence of cavitand showed no observable hemiaminal by NMR spectroscopy under the mild conditions used here. On mixing 10 mM *n*-propylamine and 1.5 mM 9-anthraldehyde, we observed only the slow formation of the imine in the NMR spectrum. At these concentrations of amine and receptor **1**, the rate of imine formation is ~50 times faster in the cavitand. In contrast to the steady state behavior that governs the formation of many reactive intermediates, the concentration of the hemiaminal in this case was seen to build up and decline over time (fig. S10). The noncovalent complex persisted at low concentration, and the ratio of hemiaminal to complex was constant after equilibrium was reached. The equilibrium constant for the internal reaction is $K \approx 12.5$.

How does the cavitand stabilize the otherwise elusive hemiaminal intermediates? Previous studies with analogous receptors (lacking the introverted aldehyde functionality) show that the cavitand folds around the amine and isolates it from the bulk solution in an ordered cage of aromatic rings and secondary amide groups (*20*, *21*). When the aldehyde function is positioned over the cavity, it is held close to the guest inside, and the reaction becomes almost intramolecular from an entropic standpoint, lowering the barrier to bond formation. The secondary amides are poised to stabilize the

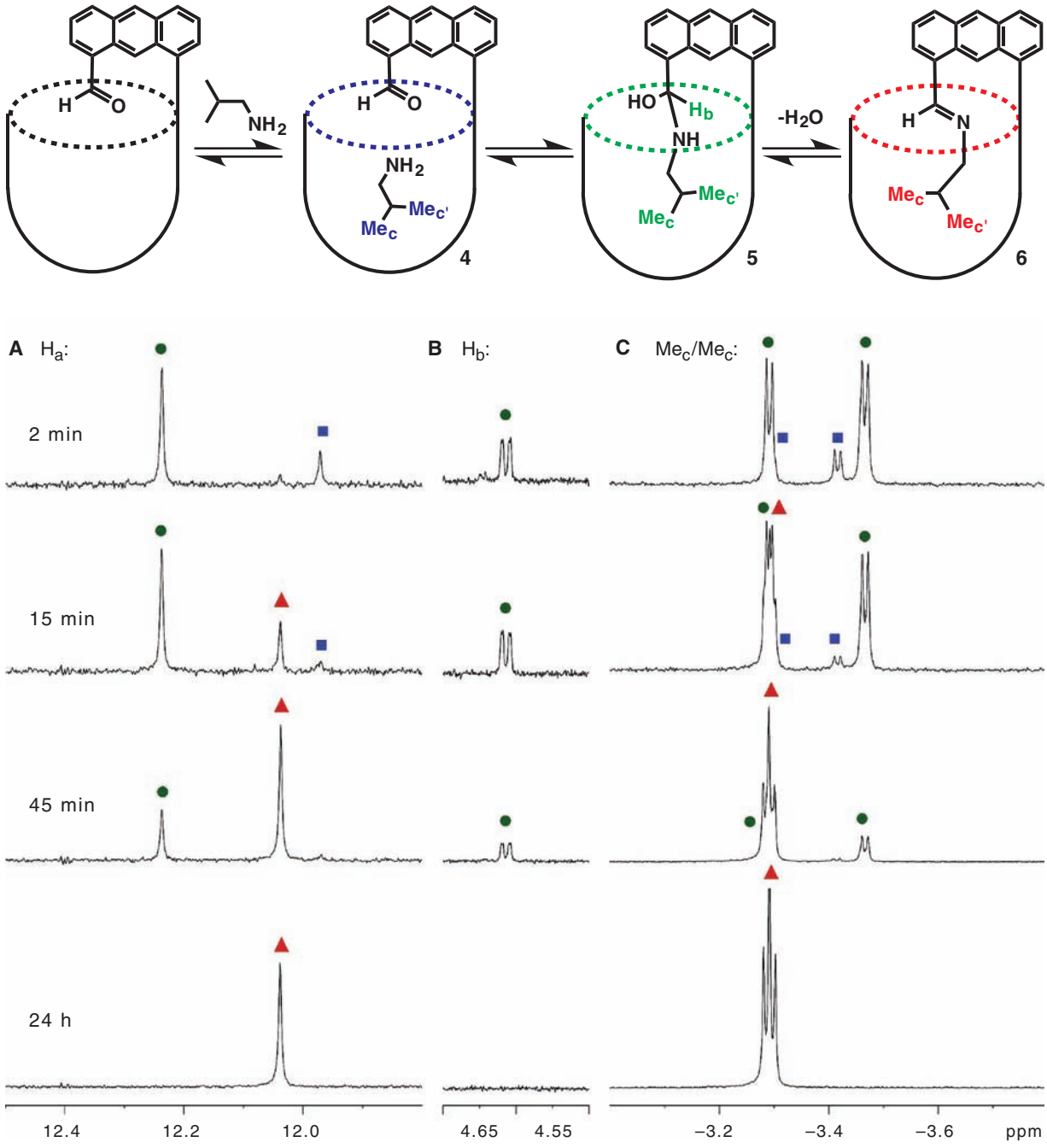

Fig. 3. The reaction in the cavitand. Representation of the reaction process and sections of the ^{1}H NMR spectra obtained upon addition of isobutylamine (10 mM) to a 1.5 mM solution of cavitand **1** in mesitylene-d_{12}. ■ host:guest complex **4**, ● hemiaminal intermediate **5**, and ▲ imine product **6**. (**A**) Downfield region showing benzimidazole proton H_a (Fig. 2); (**B**) mid-field region showing hemiaminal CH_b; (**C**) upfield region showing $Me_{C/C'}$. Me, methyl group.

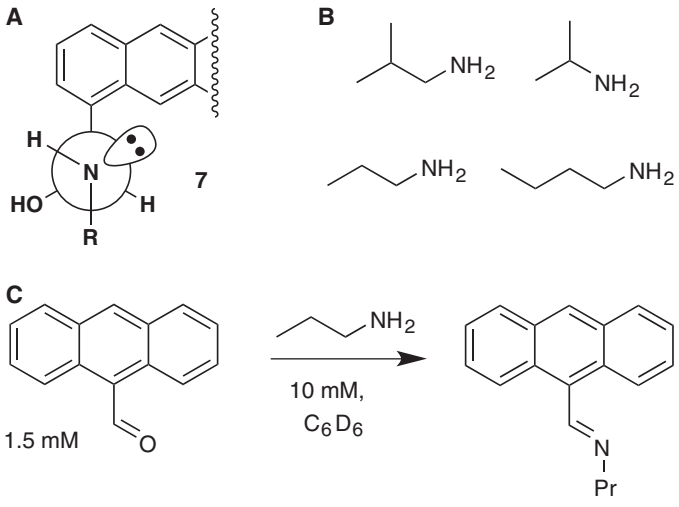

Fig. 4. (**A**) Conformation of the hemiaminal stereocenter inside the complex as viewed down the newly formed N-C bond (one of two possible enantiomers is shown); (**B**) other amines for which hemiaminal formation is observed; (**C**) representation of the cavitand-free control reaction. Pr, propyl group.

tetrahedral intermediates through hydrogen bonding, which also reduces the enthalpic price of the reaction. Accordingly, the cavitand provides a nearly ideal environment for this reaction: The reactants are confined in a limited space and properly oriented, and the desired reactive intermediate is actively stabilized. The stabilization is further enhanced by the binding of the intermediate. In free solution, the dehydration step is self-promoted; in the absence of a better base, a second amine molecule can accelerate the elimination of water. The confinement provided by the cavitand prevents interaction between external base and tetrahedral intermediate, thereby inhibiting progression to the imine.

Are these confining cavities capable of shifting equilibria toward otherwise unstable intermediates (*22*)? Enzyme-catalyzed reactions show enormous rate enhancements through binding to reaction intermediates that structurally resemble transition states. The alteration of equilibria inside enzymes such as triose phosphate isomerase has been proposed (*23*, *24*) but, despite close examination (*25*), has yet to be confirmed. Another proposal relates the magnitude of these effects to the attractive forces between enzyme and substrate, with the greatest effects arising from the formation of covalent bonds (*26*). The evidence presented here supports this view, insofar as the cavitand's functional group arrangement resembles an enzyme active site. Although these cavitands are not catalysts, they show a capacity in stoichiometric quantities to trap reactive intermediates, allowing more direct study of reaction mechanisms.

References and Notes

1. J. Rebek Jr., *Tetrahedron* **35**, 723 (1979).
2. R. I. Masel, *Chemical Kinetics and Catalysis* (Wiley-Interscience, New York, 2001).
3. E. V. Anslyn, D. A. Dougherty, in *Modern Physical Organic Chemistry* (University Science, Sausalito, CA, 2006), ch. 10.
4. D. A. Evans, G. Borg, K. A. Scheidt, *Angew. Chem. Int. Ed.* **41**, 3188 (2002).
5. L. Floriani, E. Marianucci, P. E. Todesco, *J. Chem. Res.* **1984**, 126 (1984).
6. J. A. Chudek, R. Foster, D. Young, *J. Chem. Soc., Perkin Trans. 2* 1285 (1985).
7. D. M. Rudkevich, J. Rebek Jr., *Eur. J. Org. Chem.* **1999**, 1991 (1999).
8. B. W. Purse, P. Ballester, J. Rebek Jr., *J. Am. Chem. Soc.* **125**, 14682 (2003).
9. V. M. Dong, D. Fiedler, B. Carl, R. G. Bergman, K. N. Raymond, *J. Am. Chem. Soc.* **128**, 14464 (2006).
10. M. Ziegler, J. L. Brumaghim, K. N. Raymond, *Angew. Chem. Int. Ed.* **39**, 4119 (2000).
11. M. Yoshizawa, T. Kusukawa, M. Fujita, K. Yamaguchi, *J. Am. Chem. Soc.* **122**, 6311 (2000).
12. T. Iwasawa, E. Mann, J. Rebek Jr., *J. Am. Chem. Soc.* **128**, 9308 (2006).
13. M. Kawano, Y. Kobayashi, T. Ozeki, M. Fujita, *J. Am. Chem. Soc.* **128**, 6558 (2006).
14. D. Fiedler, R. G. Bergman, K. N. Raymond, *Angew. Chem. Int. Ed.* **43**, 6748 (2004).
15. A. Heine *et al.*, *Science* **294**, 369 (2001).
16. E. Lorentzen, B. Siebers, R. Hensel, E. Pohl, *Biochemistry* **44**, 4222 (2005).
17. A. R. Renslo, J. Rebek Jr., *Angew. Chem. Int. Ed.* **39**, 3281 (2000).
18. S. Lin, L. Yang, *Tetrahedron Lett.* **46**, 4315 (2005).
19. T. Gottschalk, B. Jaun, F. Diederich, *Angew. Chem. Int. Ed.* **46**, 260 (2007).
20. R. J. Hooley, J. Rebek Jr., *J. Am. Chem. Soc.* **127**, 11904 (2005).
21. B. W. Purse, A. Gissot, J. Rebek Jr., *J. Am. Chem. Soc.* **127**, 11222 (2005).
22. A. Fersht, *Enzyme Structure and Mechanism* (Freeman, New York, 1984), pp. 47–97.
23. W. J. Albery, J. R. Knowles, *Biochemistry* **15**, 5627 (1976).
24. J. R. Knowles, *Nature* **350**, 121 (1991).
25. S. Rozovsky, A. E. McDermott, *Proc. Natl. Acad. Sci. U.S.A.* **104**, 2080 (2007).
26. X. Zhang, K. N. Houk, *Acc. Chem. Res.* **38**, 379 (2005).
27. We are grateful to the Skaggs Institute and the NIH (grant GM 50174) for financial support. T.I. and R.J.H. are Skaggs Postdoctoral Fellows.

Supporting Online Material

www.sciencemag.org/cgi/content/full/317/5837/493/DC1
Materials and Methods
Figs. S1 to S10
References

2 April 2007; accepted 31 May 2007
10.1126/science.1143272

A Powerful Chiral Counterion Strategy for Asymmetric Transition Metal Catalysis

Gregory L. Hamilton, Eun Joo Kang, Miriam Mba, F. Dean Toste*

Traditionally, transition metal–catalyzed enantioselective transformations rely on chiral ligands tightly bound to the metal to induce asymmetric product distributions. Here we report high enantioselectivities conferred by a chiral counterion in a metal-catalyzed reaction. Two different transformations catalyzed by cationic gold(I) complexes generated products in 90 to 99% enantiomeric excess with the use of chiral binaphthol–derived phosphate anions. Furthermore, we show that the chiral counterion can be combined additively with chiral ligands to enable an asymmetric transformation that cannot be achieved by either method alone. This concept of relaying chiral information via an ion pair should be applicable to a vast number of metal-mediated processes.

The preparation of enantiomerically pure compounds has become a requirement for agrochemical and pharmaceutical synthesis. Such chiral nonracemic compounds are typically accessed from either Nature's "chiral pool," by resolution of a racemate or by means of an enantioselective transformation mediated by a chiral catalyst (*1*). In general, chiral catalysts rely on covalent (dative or nondative) bonds between the reactive site and the chiral moiety. An alternative approach, which takes advantage of the fact that many enantioselective catalysts bear a positive charge, is the induction of asymmetry by interaction of the cationic catalyst with a chiral counteranion associated with the metal in an ion pair. This idea is potentially very powerful because, in principle, the same or a small library of chiral anionic counterions could be used to make a wide range of cationic catalysts enantioselective. The importance of chiral ion pairs is well known in the fields of phase-transfer catalysis (*2*) and organocatalysis (*3*–*6*) and may also be relevant to chiral Brønsted acid catalysis (*7*).

Department of Chemistry, University of California at Berkeley, Berkeley, CA 94720, USA.

*To whom correspondence should be addressed. E-mail: fdtoste@berkeley.edu